

Insights into Enzyme Reactions with Redox Cofactors in Biological Conversion of CO₂

Du-Kyeong Kang^{1,2}, Seung-Hwa Kim^{1,2}, Jung-Hoon Sohn^{1,2}, and Bong Hyun Sung^{1,2*}

¹*Synthetic Biology Research Center, Korea Research Institute of Bioscience and Biotechnology (KRIBB), Daejeon 34141, Republic of Korea*

²*Department of Biosystems and Bioengineering, Korea University of Science and Technology (UST), Daejeon 34113, Republic of Korea*

Carbon dioxide (CO₂) is the most abundant component of greenhouse gases (GHGs) and directly creates environmental issues such as global warming and climate change. Carbon capture and storage have been proposed mainly to solve the problem of increasing CO₂ concentration in the atmosphere; however, more emphasis has recently been placed on its use. Among the many methods of using CO₂, one of the key environmentally friendly technologies involves biologically converting CO₂ into other organic substances such as biofuels, chemicals, and biomass via various metabolic pathways. Although an efficient biocatalyst for industrial applications has not yet been developed, biological CO₂ conversion is the needed direction. To this end, this review briefly summarizes seven known natural CO₂ fixation pathways according to carbon number and describes recent studies in which natural CO₂ assimilation systems have been applied to heterogeneous *in vivo* and *in vitro* systems. In addition, studies on the production of methanol through the reduction of CO₂ are introduced. The importance of redox cofactors, which are often overlooked in the CO₂ assimilation reaction by enzymes, is presented; methods for their recycling are proposed. Although more research is needed, biological CO₂ conversion will play an important role in reducing GHG emissions and producing useful substances in terms of resource cycling.

Keywords: CO₂ assimilation, CO₂-fixation pathway, C1 reduction, redox cofactor, synthetic biology

Introduction

Net-zero carbon emission is a worldwide task owing to the rapidly increasing greenhouse gas (GHG) levels in the atmosphere. Among the human-made GHGs, C1 molecules, especially carbon dioxide (CO₂), are receiving considerable attention as they account for almost 70% of the GHGs that are contributing to the rapidly intensifying global warming and climate change [1]. The CO₂ concentration in the atmosphere has markedly increased since the Industrial Revolution and is now almost 50% higher than preindustrial levels, at 412 parts per million (ppm) on average. Global surface temperatures have increased, in correlation with atmospheric concentrations of CO₂, by nearly 1°C compared to preindustrial levels [2, 3]. This increase of 1°C has caused a number of distinct changes, including higher temperatures on land and in the oceans, glacier melting, and increased frequency and severity of precipitation or drought. Furthermore, many experts have predicted that these changes will become more severe with a global warming of 1.5°C over preindustrial levels and that the damages will be difficult to reverse at 2°C of global warming [4]. In addition to climate change, rising atmospheric concentrations of GHGs have the potential to threaten ecosystems and eventually affect humans adversely [5-7]. Therefore, to maintain global temperatures below 1.5°C, efforts to achieve a phased goal of reducing carbon emissions by 45% from 2005 to 2030 and eventually reaching net-zero carbon emissions by 2050 are desperately needed [8]. Solving the problem of the CO₂ in the atmosphere is not only an environmental issue but also provides the opportunity to use a substrate on which the carbon skeleton of profitable materials, such as fuels and various chemicals, can be built. Therefore, more attention is now being paid to CO₂ sequestration with reference to carbon capture, utilization, and storage (CCUS) than to carbon capture and storage (CCS). Carbon storage technology involves capturing the carbon in the atmosphere and transporting carbon gases underground, typically using geological space as a carbon storage reservoir. Studies on CCS technology using industrial solid waste and steel-making slags, as carbon storage, are ongoing [9-11]. CCUS technology involves carbon capture and utilization to generate value-added products through subsequent reactions [12]. Biological CO₂ reduction or assimilation, which will be introduced in this paper, is included in the CCUS in terms of generating biomass and valuable materials.

Studies on the mitigation and use of CO₂ are being conducted in various applications such as metal- and nanomaterials-fused electrochemical catalysis, photocatalysis, and biological catalysis [13-15]. Among these,

Received: June 5, 2023
Accepted: June 12, 2023

First published online:
June 26, 2023

*Corresponding author
Phone: +82-42-860-4472
Fax: +82-42-879-4458
E-mail: bhsung@kribb.re.kr

pISSN 1017-7825
eISSN 1738-8872

Copyright © 2023 by the authors.
Licensee KMB. This article is an
open access article distributed
under the terms and conditions
of the Creative Commons
Attribution (CC BY) license.

biological CO₂ conversion is an environmentally friendly and highly substrate-specific and reusable method that recycles CO₂ substrates into value-added products. Ecosystems can efficiently reduce CO₂ emissions through biological CO₂ assimilation, which can be performed by plants and microorganisms. However, the large amounts of CO₂ gases emitted by human activities have already exceeded the assimilation capacity of the natural ecosystem, causing excessive global warming [16]. To increase the carbon fixation efficiency beyond that of natural cycles, novel biotechnologies, such as synthetic biology, need to be incorporated into natural biological carbon reduction systems. Therefore, biomimetic strategies such as rebuilding paths by introducing partial heterologous carbon fixation pathways into *in vivo* and *in vitro* models may be crucial in solving the carbon fixation problem. In this review, we briefly provide an overview of the natural CO₂ fixation pathways with enzymes and cofactors and introduce the application of biological CO₂ assimilation studies. In addition, we discuss the cofactors called redox partners, which are essential components that play important roles in regulating C1 fixation. Our aim with this review was to provide a better understanding of the overall biological CO₂ fixation pathways in nature, including not only C1-converting enzymes but also their important redox cofactors in CO₂ reduction, and to represent novel possibilities for biological C1 fixation.

CO₂ Fixation Pathways in Nature

To date, seven carbon fixation pathways have been identified in nature. Each pathway can assimilate different types of C1, such as gaseous CO₂ and bicarbonate (HCO₃⁻). The Calvin–Benson–Basham (CBB), Wood–Ljungdahl pathway (WLP), reductive glycine pathway (rGlyP), and reductive tricarboxylic acid cycle (rTCA) can fix gaseous CO₂, whereas 3-hydroxypropionate (3-HP) bicycle and 3-hydroxypropionate/4-hydroxybutyrate (3-HP/4-HB) cycle can fix bicarbonate. Both forms of carbon can be assimilated in the dicarboxylate/4-hydroxybutyrate (DC/4-HB) cycle. All pathways except the CBB cycle involve acetyl-CoA. A comprehensive representation of all natural CO₂ fixation pathways is depicted in Fig. 1 based on the carbon number. The carbon-fixing enzymes and cofactors are listed in Table 1, along with their carbon-assimilating reaction and simplified change in carbon number.

The CBB cycle, also known as the reductive pentose phosphate cycle, is the predominant carbon fixation pathway in plants and photosynthetic bacteria. In this cycle, CO₂ and water are converted into organic compounds using cofactors such as light-driven ATP and NADPH [17]. The key enzyme used for CO₂ fixation in the CBB cycle is ribulose-1,5-bisphosphate carboxylase/oxygenase (RuBisCO), which is categorized as a lyase. RuBisCO catalyzes the addition of CO₂ to ribulose 1,5-bisphosphate (C5) and splits into two molecules of 3-phosphoglycerate (C3).

The WLP is one of the noncyclic pathways among the seven natural carbon fixation pathways and is also

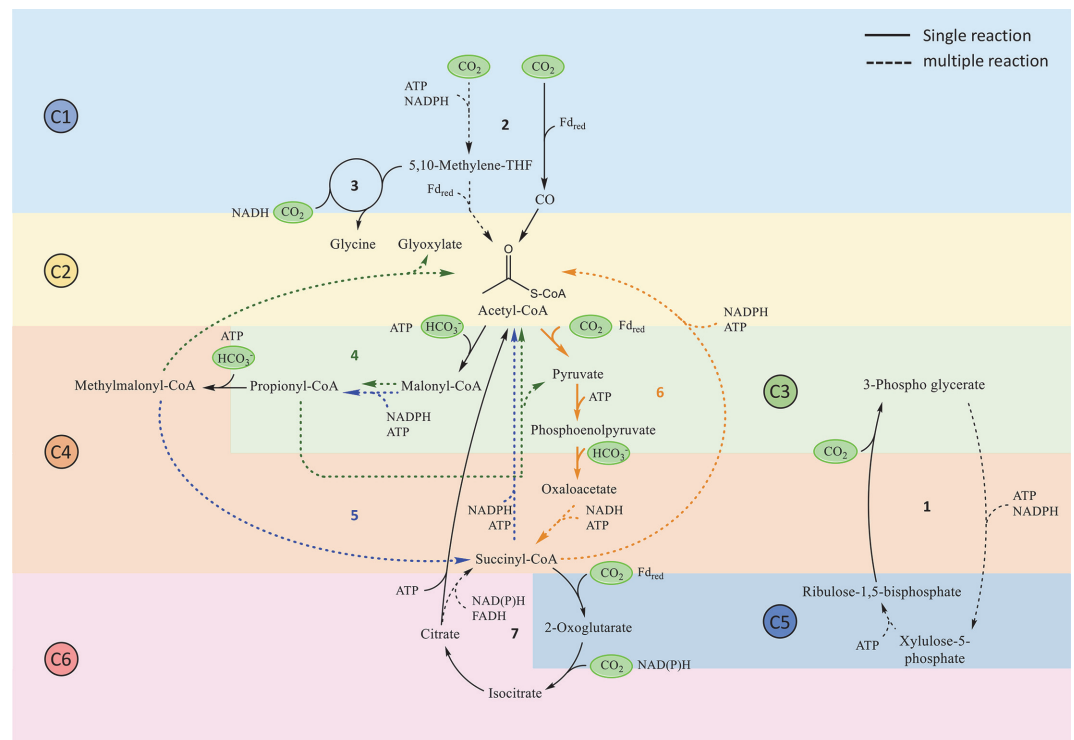


Fig. 1. An overview illustration of major CO₂ assimilation pathways in nature. (1) Calvin-Benson-Basham cycle; (2) Wood-Ljungdahl pathway; (3) reductive glycine pathway; (4) 3-hydroxypropionate bicycle; (5) 3-hydroxypropionate/4-hydroxybutyrate cycle; (6) dicarboxylate/4-hydroxybutyrate cycle; and (7) reductive citric acid cycle. The 3-HP bicycle, 3-HP/4-HB cycle, and DC/4-HB cycle are represented by green, blue, and orange lines, respectively.

Table 1. Natural CO₂ assimilation pathways.

Name of pathway	Enzymes (EC Number)	CO ₂ fixation reaction	Simplified reaction	Cofactor requirements	Ref
Calvin-Benson-Bassham cycle (CBB)	Rubisco (4.1.1.39)	Ribulose-1,5-bisphosphate + CO ₂ → 3-Phosphoglycerate	C5 + C1 → 2C3	-	[17]
Wood-Ljungdahl pathway (WLP)	Formate dehydrogenase (1.17.1.9) Carbon monoxide dehydrogenase (1.2.7.4)	CO ₂ + NADPH → Formate CO ₂ + Fd _{red} → CO	C1 → C1 C1 → C1	NADPH reduced Fd	[18]
reductive glycine pathway (rGlyP)/ Glycine cleavage/synthase system (GCS)	Aminomethyltransferase (2.1.2.10) Glycine dehydrogenase (1.4.4.2) Dihydropyridyl dehydrogenase (1.8.1.4)	5,10-methylene-THF + NH ₃ + CO ₂ + NADH → Glycine + THF + NAD ⁺	One carbon unit + C1 → C2	NADH	[74]
3-Hydroxypropionate bicycle (3HP)	Acetyl-CoA carboxylase (6.4.1.2) Propionyl-CoA carboxylase (6.4.1.3)	Acetyl-CoA + HCO ₃ ⁻ + ATP → Malonyl-CoA + ADP Propionyl-CoA + HCO ₃ ⁻ + ATP → (s)-Methylmalonyl-CoA + ADP	C2-CoA + C1 → C3-CoA C1 → C4-CoA	ATP ATP	[25]
3-Hydroxypropionate/4-Hydroxybutyrate cycle (3HP/4HB)	Acetyl-CoA carboxylase (6.4.1.2) Propionyl-CoA carboxylase (6.4.1.3)	Acetyl-CoA + HCO ₃ ⁻ + ATP → Malonyl-CoA + ADP Propionyl-CoA + HCO ₃ ⁻ + ATP → (s)-Methylmalonyl-CoA + ADP	C2-CoA + C1 → C3-CoA C1 → C4-CoA	ATP ATP	[28]
Dicarboxylate/4-Hydroxybutyrate cycle (DC/4HB)	Pyruvate synthase (1.2.7.1) Phosphoenolpyruvate carboxylase (4.1.1.31)	Acetyl-CoA + CO ₂ + Fd _{red} → Pyruvate + Fd _{oxi} Phosphoenolpyruvate + HCO ₃ ⁻ → Oxaloacetate	C2-CoA + C1 → C3 C3 + C1 → C4	Reduced Fd -	[26]
reverse Tricarboxylic acid cycle (rTCA)	2-Oxoglutarate oxidoreductase (1.2.7.3) Isocitrate dehydrogenase (6.4.1.7)	Succinyl-CoA + CO ₂ + Fd _{red} → 2-Oxoglutarate + Fd _{oxi} 2-Oxoglutarate + CO ₂ + NAD(P)H → Isocitrate + NAD(P) ⁺	C4 + C1 → C5 C5 + C1 → C6	Reduced Fd NAD(P)H	[29]

denoted as the reductive acetyl-CoA route. In this pathway, CO₂ molecules are reduced into formate and carbon monoxide (CO) via formate dehydrogenase (FDH) and CO dehydrogenase in the initial stage, respectively. In this pathway, two molecules of CO₂ are converted into one molecule of acetyl-CoA (C2) using cofactors such as NADPH, ATP, and reduced ferredoxin (Fd_{red}) [18].

The rGlyP is a CO₂ fixation metabolic pathway found in anaerobic bacteria, eukaryotes, and plants [19-21]. The initial reaction in this pathway starts with reducing CO₂ to formate or directly reducing formate to 10-formyltetrahydrofolate (10-formyl-THF) [22]. The subsequent reactions of 10-formyl-THF produce 5,10-methylene-THF, which is used as a one-carbon unit for attaching additional CO₂ to produce glycine. This process is catalyzed by a multienzyme complex called the glycine cleavage/synthase system (GCS), consisting of aminomethyltransferase, glycine dehydrogenase, and dihydropyridyl dehydrogenase [23]. To assimilate CO₂ into 5,10-methylene-THF to generate glycine (C2), NADH and NH₃ are required as cofactors [24].

The 3-HP bicycle was discovered in the thermophilic green nonsulfur bacteria, *Chloroflexus aurantiacus*, which obtains energy from light. In this cycle, two molecules of bicarbonate are fixed by acetyl-CoA carboxylase and propionyl-CoA carboxylase, and these enzymes generate C3 and C4 products, respectively, in the presence of ATP. The initial step of the 3-HP cycle is the conversion of acetyl-CoA (C2) to malonyl-CoA (C3) by acetyl-CoA carboxylase; after sequential steps, propionyl-CoA (C3) is converted into methylmalonyl-CoA (C4) by propionyl-CoA carboxylase [25]. In the last step of the 3-HP cycle, methyl-CoA, made from methylmalonyl-CoA, is split into acetyl-CoA and glyoxylate; (s)-citramalyl-CoA, which is formed through several steps after combining glyoxylate and propionyl-CoA, is divided into acetyl-CoA and pyruvate.

The 3-HP/4-HB cycle is a carbon fixation pathway that was discovered in *Sulfolobales* such as *Metallosphaera* and *Thaumarchaeota* [26,27]. The cycle starts with the conversion of acetyl-CoA (C2) into malonyl-CoA (C3) by incorporating bicarbonate; then, following sequential steps, propionyl-CoA (C3) is carboxylated to succinyl-CoA

(C4) through methylmalonyl-CoA (C4) by incorporating additional bicarbonate. The key enzyme of inorganic carbon assimilation is acetyl-CoA/propionyl-CoA carboxylase, which generates two acetyl-CoA molecules from one acetyl-CoA, with 3-HP and 4-HB as key intermediates [28]. In this pathway, NADPH and ATP function as essential cofactors for the production of methylmalonyl-CoA from acetyl-CoA.

The DC/4-HB cycle was discovered in the anaerobic hyperthermophilic archaea, *Ignicoccus* species, which use CO₂ with sulfur and hydrogen for their growth. CO₂ is assimilated via acetyl-CoA to pyruvate using reduced ferredoxin (Fd_{red}) by pyruvate synthase, and bicarbonate is transformed into phosphoenolpyruvate to oxaloacetate by phosphoenolpyruvate carboxylase. The cofactors needed for C1 assimilation in this pathway include reduced Fd, ATP, and NAD(P)H [26].

The rTCA cycle is the reverse of the TCA cycle, so is also called the reverse TCA cycle. In this cycle, two molecules of CO₂ are formed as C6 products from a C4 material through two steps. The first step involves catalysis by 2-oxoglutarate oxidoreductase, which produces 2-oxoglutarate (C5) from succinyl-CoA (C4) using one molecule of CO₂ and the reducing energy from Fd_{red}. In the second step, isocitrate dehydrogenase provides CO₂ fixation into 2-oxoglutarate (C5) to generate isocitrate (C6) [29]. Cofactors such as NAD(P)H, ATP, Fd_{red}, and FADH are used in rTCA cycle. In addition, the model in which isocitrate lyase is introduced has the shortest pathway to reduce two molecules of CO₂ per cycle [30, 31]. The key elements of these CO₂ fixation pathways are heterologously expressed and used in model microorganisms.

In Vivo Applications of Natural Biological CO₂ Assimilation Systems

Many in vivo heterologous assimilation studies have been conducted to adapt metabolic pathways to use CO₂. RuBisCO, which is involved in the CBB cycle, has been extensively studied to generate microorganisms with a non-native CBB cycle for CO₂ fixation. Hence, diverse approaches have been considered for constructing CO₂ assimilation bio-platforms using various techniques, such as genetic modification, strain evolution, and computational analyses of metabolic flux. For CO₂ fixation, *Escherichia coli* was rewired to supply ATP and NADH from pyruvate through the TCA cycle as an energy module, fixing CO₂ by RuBisCO as an assimilation module [32]. To strengthen the CO₂ fixation ability of the strain that introduces RuBisCO and phosphoribulokinase, laboratory evolution and computational analyses were conducted, which resulted in an autotroph strain that has the ability to use CO₂ for biomass under higher CO₂ concentrations than the ancestral strain [33]. Similar to the two-module system study, autotrophic *E. coli* engineered with RuBisCO and FDH was constructed to convert CO₂ to all-carbon biomass while regenerating cofactors such as NADH and ATP [34]. In addition to introducing only RuBisCO, researchers have reduced exogenous and endogenous CO₂ by introducing the CBB operon from *Rhodobacter sphaeroides* and 20 heterologous genes related to CO₂-concentrating mechanisms into *E. coli* [35, 36]. The ribulose-monophosphate (RuMP) pathway catalyzes the conversion of formaldehyde derived from CO₂ or methane into biomass. Activating sedoheptulose biphosphatase in RuMP pathway into *E. coli* led to three-fold-enhanced formaldehyde incorporation ability [37]. In addition, *E. coli* with a reconstructed metabolic pathway into which a RuMP shunt was introduced effectively converted methanol and sarcosine-derived formaldehyde into biomass [38]. RuMP-introduced methylotrophic *E. coli* was developed via flux balance analysis [39]. Furthermore, studies on converting C1 substances such as methanol, formate, and CO₂ into various products via a modified serine cycle and rGlyP have also been conducted [40-42]. Carbonic anhydrase (CA), an enzyme that can directly convert CO₂ to the ionic form of bicarbonate (HCO₃⁻), was used to construct *E. coli* that could produce an industrially attractive material, calcium carbonate (CaCO₃) [43].

Other bio-platforms for *E. coli* have also been studied for CO₂ fixation. Cyanobacteria, which are representative photosynthetic marine bacteria, have been extensively studied for their ability to produce various biochemicals and biofuels while fixing CO₂. RuBisCO in cyanobacteria was used as a CO₂-fixing module and oleochemical-producing modules were added. A strain overexpressing the efflux pump and deficient *aas* gene coding for acyl-acyl carrier protein (acyl-ACP) demonstrated a high free fatty acid (FFA) content of 640 mg/l [44]. Another mutant introducing thioesterase A and fatty acid photodecarboxylase with acyl-ACP deficient *Synechocystis* sp. produced 111.2 mg/l of fatty alkanes [45]. In addition, *Synechocystis* sp., lacking the acyl-ACP synthetase gene (*Δaas*) and overexpressing the genes *sfp* and *car* encoding phosphopantetheinyl transferase and carboxylic acid reductase, respectively, produced over 905 mg/l of 1-octanol from CO₂ [46].

In vitro Studies of Biological CO₂ Assimilation

Various in vitro enzymatic CO₂ reductions have been studied by investigating and exploring novel biocatalysts, further engineering wild-type enzymes, optimizing reaction conditions, introducing cascade systems, and immobilizing enzymes to increase C1 assimilation efficiencies. Researchers have produced methanol from CO₂ through formate and formaldehyde using FDH, formaldehyde dehydrogenase (FaldH), and alcohol dehydrogenase enzymes. The representative CO₂ reduction enzyme FDH, which produces formate from CO₂, has been extensively studied. A newly discovered FDH from *Thiobacillus* sp. (TsFDH) has approximately 85-fold higher activity in reducing CO₂ than the FDH from *Candida boidinii*, which is commercially available but has weak CO₂ reduction activity [47]. Following this study, other FDHs have continuously been discovered from new species, such as *Candida methylica*, *Chaetomium thermophilum*, and *Rhodococcus jostii*, and examined for CO₂ reduction [48, 49]. In addition, the introduction of a multienzyme cascade reaction with a cofactor regeneration system and the optimization of C1 reduction conditions using novel FaldH from *Burkholderia multivorans* showed up to 500-fold increased methanol production from CO₂ compared to that of other systems [50]. Moreover, biochemical approaches involving the introduction of conductive polyaniline hydrogels and nanobiocatalysts, which are

graphene-immobilized enzymes, have increased CO₂ conversion efficiency [51, 52].

Studies on producing materials other than methanol from CO₂ have also been conducted. A novel CA from *Corynebacterium flavescens* in cow saliva was isolated, which produced up to 45 mg CaCO₃/mg protein from CO₂ through the optimization of the reaction parameters [53]. Another dehydrogenase involved in the rTCA cycle, isocitrate dehydrogenase from *Chlorobium limicola*, which can assimilate CO₂ to 2-oxoglutarate, was characterized [54]. In addition to dehydrogenases for CO₂ fixation, various oxidoreductases, such as pyruvate:ferredoxin oxidoreductase (PFOR), oxalate oxidoreductase (OOR), 2-oxoglutarate:ferredoxin oxidoreductase (OGOR), and other 2-oxoacid:ferredoxin oxidoreductases (OFORs), whose reactions are mediated by Fd as the electron mediator, have been explored. The function of CO₂ fixation in these OFORs has been identified and analyzed based on model structures [55-57]. Efforts to discover highly active CO₂ sequestering enzymes are ongoing.

Redox Cofactors and Cofactor Recycling

Not only enzymes but also redox cofactors that supply reducing power and energy play an important role in biological CO₂ assimilation [58, 59]. Even for enzymes with reversible activity, cases exist in which one direction is

Table 2. Representative biological and chemical redox cofactors.

Group	Type of electron carrier	PDB ID	Prosthetic groups	Redox potential (mV)	Condition	Ref
Redox couples	NAD ⁺ /NADH			-320	pH 7.0	[75]
	NADP ⁺ /NADPH			-320	pH 7.0	[75]
	FMN/FMNH ₂			-380	pH 7.0	[76]
Ferredoxins	FAD/FADH ₂			-208	pH 7.0, 25°C	[77]
	AlvinFd	1BLU	2[4Fe-4S]	-467, -640	pH 7.0	[78]
	AvFd	6FD1, 7FD1	[3Fe-4S], [4Fe-4S]	-420, -650	pH 7.0, 0°C	[78] [79]
	BpFd	ND	1[4Fe-4S]	-390	pH 6.0 to 7.5	[80]
	BtFdI/II	1IQZ/1IRO	1[4Fe-4S]	ND	ND	[81]
	CaFd	1FCA, 2FDN	2[4Fe-4S]	ND	ND	[81]
	ClFd	ND	2[4Fe-4S]	<-500	ND	[58]
	CpFd	1CLF	2[4Fe-4S]	-420	pH 7.0	[78]
	CtFdI/II	ND	2[4Fe-4S]	-514/-584	pH 7.5, at 25°C	[82]
	CvFd	1BLU	2[4Fe-4S]	-461, -653	pH 7.5, at 25°C	[83]
	DaFdI	1FXR, 1DAX	1[4Fe-4S]	-385	pH 7.0, at 23°C	[81]
	EcFd	2ZVS	2[4Fe-4S]	-418, -675	pH 7.0	[84]
	EhFd	ND	2[4Fe-4S]	-333	pH 7.0	[84]
	HtFd1	7M1N	1[4Fe-4S]	-485	pH 7.0, at 23°C	[59]
	MmFd1/2/3	ND	2[4Fe-4S]	-485, -635/-520/-233, -380	pH 7.0	[57]
	MtFd	ND	2[4Fe-4S]	-454, -487	pH 7.6	[85]
	PaFd	2FGO	2[4Fe-4S]	-475, -655	pH 7.0	[81]
	SaFd	ND	[3Fe-4S], [4Fe-4S]	-275, -529	pH 6.4, 0°C	[86]
	TaFd	1RGV	2[4Fe-4S]	-431, -587	pH 7.0, 0°C	[87]
	TmFd	1VJW, 1ROF	2[4Fe-4S]	-420	pH 7.0, 0°C	[81]
TtFd	1H98	[3Fe-4S], [4Fe-4S]	ND	ND	[81]	
Pyridine	Benzyl viologen			-578.2/-745.4	pH 7.4, 25°C	[88]
	Ethyl viologen			-701.5/-992.3	pH 7.4, 25°C	
	Methyl viologen			-697.5/-1029.5	pH 7.4, 25°C	
	1,1'-Diheptyl-4,4'-bipyridinium			-626.2/-786.2	pH 7.4, 25°C	
	1,1'-Diphenyl-4,4'-bipyridinium			-457.5	pH 7.4, 25°C	
	4,4'-Dipyridyl			-1080	pH 7.4, 25°C	
	1-Heptyl-4-(4-pyridyl)pyridinium			-949	pH 7.4, 25°C	
	2-Hydroxy-1,4-naphthoquinone			-535.4	pH 7.4, 25°C	
Quinone	2-Methyl-1,4-Naphthoquinone			-411.7	pH 7.4, 25°C	

Abbreviations: Alvin: *Allochroamium vinosum*; Av: *Azotobacter vinelandii*; Bp: *Bacillus polymyxa*; Bt: *Bacillus thermoproteolyticus*; Ca: *Clostridium acidurici*; Cl: *Chlorobium limicola*; Cp: *Clostridium pasteurianum*; Ct: *Chlorobium tepidum*; Cv: *Chromatium vinosum*; Da: *Desulfovibrio africanus*; Ec: *Escherichia coli*; Eh: *Entamoeba histolytica*; Ht: *Hydrogenobacter thermophiles*; Mm: *Magnetococcus marinus*; Mt: *Moorella thermoacetica*; Pa: *Pseudomonas aeruginosa*; Sa: *Sulfolobus acidocaldarius*; Ta: *Thauera aromatica*; Tm: *Thermotoga maritima*; Tt: *Thermus thermophiles*; ND: not determined.

more dominant than the other in general; notably, C1 fixation/reduction bias is more challenging than the reverse reaction. To overcome the thermodynamic barriers between substances, most carbon-fixing enzymes must receive electrons, either directly or through cofactors, which provide the driving force to reduce the C1 molecule. Therefore, the enzymes directly involved in carbon conversion are key elements, and the cofactors that promote enzymatic reactions are also critical to the overall reaction. A redox cofactor is essential for redox equivalence in terms of the electron carriers or mediators in efficient CO₂ assimilation reactions. It takes and provides an electron or energy to other proteins depending on the driving force. The biological and chemical redox cofactors and their potentials are listed in Table 2. Some representative biological electron cofactors are NAD(P)⁺/NAD(P)H and Fd; ring-form materials, such as pyridine, quinone, and aniline, are used as chemical redox cofactors [60]. Among the chemical redox cofactors, viologen derived from 4,4'-bipyridine is widely used as a chemical electron mediator [61]. For example, CO₂ is converted into carbon monoxide and formic acid at reduction potentials of -596 and -417 mV, respectively. To promote CO₂ conversion, the redox cofactors with lower potential values than the -596 and -417 mV, including bipyridines, EcFd, and others, as listed in Table 2, can be applied to the CO₂ reduction reaction [62]. These cofactors work as electron donors or acceptors, and the reaction can be sustained by regenerating cofactors. Cofactor regeneration is a stable and sustainable method for CO₂ conversion that is cost-effective and highly productive [50]. Hence, the oxidized form of cofactors into the reduced form following C1 fixation must be reproduced for them to continuously act in cofactor-dependent enzymatic reactions. The CO₂-to-methanol pathway, which is a representative C1 conversion pathway, usually requires NADH as a cofactor for C1 reduction. In each step of hydrogenation, C1 substances are reduced using the reducing power generated by NADH oxidation. NADH is regenerated while converting glutamate into 2-oxoglutarate by applying glutamate dehydrogenase to recycle NAD⁺ generated in C1 reduction [63-65]. In addition, other enzymes, such as glucose dehydrogenase and xylose dehydrogenase, that use NAD/NADH can also be used as recycling cofactors [66]. Other dehydrogenases, such as glycine dehydrogenase (GlyDH) and phosphite dehydrogenase (PTDH), catalyze glycine to glyoxylate and phosphite to phosphate for NADH regeneration [50, 67]. Moreover, these cofactor regeneration enzymes, PTDH and GlyDH, have optimal activities at neutral and basic pH, respectively [67]. This means that the cofactor regeneration system can be efficiently controlled according to pH.

Another breakthrough in cofactor regeneration was the application of a hybrid system with biological or chemical materials and electrochemicals [51, 68]. The use of electric power to replenish redox cofactors or provide a direct electron supply to biocatalysts is a robust and efficient approach. In the study of carbon conversion with cofactor regeneration via electrodes, diverse materials, both biological and chemical, can act as electron carriers; some systems that do not require an electron carrier can directly transfer electrons to biocatalysts. Regenerating NAD⁺ through an electrode with a continuous supply of electrons and conjugating FDH to a polydopamine-based bioelectrode film called PDA leads to the effective reduction of CO₂ into formate [69]. Similar to the FDH-PDA bioelectrochemical method, an FDH-polyaniline hydrogel hybrid electrode was applied for effective CO₂ reduction to provide a steady electron supply [51].

Studies into chemical redox polymers, such as cobaltocene-poly(allylamine), which function as electron mediators, have led to successful CO₂ reduction through a continuous supply of electrons [70]. In the case of NAD-independent FDH, a sufficient amount of electrons provided by the electrode is transferred to the active site of FDH via iron-sulfur clusters to reduce CO₂ [71]. Chemical materials, such as cobaltocene/cobaltocenium, were also used as electron mediators and recycled by electrodes to produce H₂, CH₄, C₂H₄, and C₃H₆ from H⁺ and CO₂ [72]. In another study, for a chemical electron mediator, TiO₂ was applied to carbon monoxide dehydrogenase. CO₂ photoreduction was achieved by introducing silver nanoclusters, an electron-generating system that acts as a photosensitizer and an electron donor [73].

Conclusions and Perspectives

Biological and biomimicked CO₂ conversion is an important and promising field in terms of reducing GHGs and generating value-added materials from CO₂ or methane. Until the discovery of a novel reductive glycine pathway in 2020, six CO₂ fixation pathways were known from photoautotrophic and chemoautotrophic microorganisms. As such, more pathways to CO₂ fixation metabolism may exist. Therefore, efforts to identify new strains hold promise for discovering novel pathways that can use C1. This will lead to the possibility of discovering enzymes with enhanced C1 reduction activity or finding novel C1 fixation pathway enzymes and cofactors that can convert C1. However, issues such as the energy difference between the substrates and products remain challenging to overcome in the quest for efficient carbon assimilation. To overcome these obstacles, we need to not only intensively study the native enzymes directly involved in C1 assimilation but also improve their C1 reduction activity and sustainability through mutant studies using synthetic biology techniques. Additionally, we must build heterologous detour pathways, optimize reaction conditions, and conduct studies on cofactors that help the carbon utilization reaction. Furthermore, convergence studies must be conducted between biology and other fields, such as electrochemistry and nanomaterials, from various perspectives to increase the efficiency of C1 reduction. Biological C1 conversion shows promise as a sustainable and efficient method for converting CO₂ into valuable chemicals; however, further research and development are necessary for its widespread use. Therefore, the field of biological C1 assimilation has considerable potential in various application fields, and continuous research in this field will considerably contribute to fulfilling the global goal of net-zero carbon emissions by reducing GHG emissions and improving carbon resource recycling.

Acknowledgments

This study was supported by National Research Foundation of Korea (NRF) grants (2022M3J5A1056169, 2021M3A9I5023254, 2019R1A2C1090726, and 2018M3A9H3024746), a National Research Council of Science & Technology grant (No. CAP20023-200) by the Korean government (MSIT), and the Research Initiative Program of KRIBB (KGM5402322).

Author Contributions

All the authors contributed to writing the manuscript.

Conflict of Interest

The authors have no financial conflicts of interest to declare.

Abbreviation

CO ₂	Carbon dioxide
CO	Carbon monoxide
GHG	Greenhouse gases
CCUS	Carbon capture, utilization, and storage
CCS	Carbon capture and storage
CBB	Calvin-Benson-Basham
WLP	Wood-Ljungdahl pathway
rGlyP	Reductive glycine pathway
rTCA	Reductive tricarboxylic acid cycle
3-HP	3-hydroxypropionate
4-HB	4-hydroxybutyrate
DC	Dicarboxylate
RuBisCO	Ribulose-1,5-bisphosphate carboxylase/oxygenase
FDH	Formate dehydrogenase
Fd	Ferredoxin
10-formyl-TDF	10-formyl-tetrahydrofolate
GCS	Glycine cleavage synthase system
MV	Methyl viologen
PFOR	Pyruvate ferredoxin oxidoreductase
OOR	Oxalate oxidoreductase
OGOR	Oxoglutarate ferredoxin oxidoreductase

References

- Masson-Delmotte V, Zhai P, Pirani A, Connors SL, Péan C, Berger S, *et al.* 2021. IPCC, 2021: Summary for Policymakers. In: Climate Change 2021: The Physical Science Basis. Contribution of Working Group I to the Sixth Assessment Report of the Intergovernmental Panel on Climate Change.
- Lindsey R, Dahlman L. 2023. Climate Change: Global Temperature. *National Oceanic and Atmospheric Administration*.
- Lindsey R. 2022. Climate Change: Atmospheric Carbon Dioxide. *National Oceanic and Atmospheric Administration*.
- Hoegh-Guldberg O, Jacob D, Taylor M, Bindi M, Brown S, Camilloni I, *et al.* 2018. Impacts of 1.5°C Global Warming on Natural and Human Systems. *IPCC Special Report*.
- Larcombe AN, Papini MG, Chivers EK, Berry LJ, Lucas RM, Wyrwoll CS. 2021. Mouse lung structure and function after long-term exposure to an atmospheric carbon dioxide level predicted by climate change modeling. *Environ. Health Perspect.* **129**: 17001.
- McLean MJ, Mouillot D, Goascoz N, Schlaich I, Auber A. 2019. Functional reorganization of marine fish nurseries under climate warming. *Glob. Chang. Biol.* **25**: 660-674.
- Tabari H. 2020. Climate change impact on flood and extreme precipitation increases with water availability. *Sci. Rep.* **10**: 13768.
- Vats G, Mathur R. 2022. A net-zero emissions energy system in India by 2050: An exploration. *J. Clean. Prod.* **352**: 131417.
- Chu S. 2009. Carbon capture and sequestration. *Science* **325**: 1599.
- Zhang Y, Yu L, Cui K, Wang H, Fu T. 2023. Carbon capture and storage technology by steel-making slags: recent progress and future challenges. *Chem. Eng. J.* **455**: 140552.
- Vercelli S, Anderlucchi J, Memoli R, Battisti N, Mabon L, Lombardi S. 2013. Informing people about CCS: a review of social research studies. *Energy Procedia* **37**: 7464-7473.
- Al-Mamoori A, Krishnamurthy A, Rownaghi AA, Rezaei F. 2017. Carbon capture and utilization update. *Energy Technol.* **5**: 834-849.
- Derrick JS, Loipersberger M, Chatterjee R, Iovan DA, Smith PT, Chakarawet K, *et al.* 2020. Metal-ligand cooperativity via exchange coupling promotes iron-catalyzed electrochemical CO₂ reduction at low overpotentials. *J. Am. Chem. Soc.* **142**: 20489-20501.
- Zhang X, Guo SX, Gandionco KA, Bond AM, Zhang J. 2020. Electrocatalytic carbon dioxide reduction: from fundamental principles to catalyst design. *Mater. Today Adv.* **7**: 10074.
- Sahoo A, Chowdhury AH, Manirul Islam S, Bala T. 2022. Successful CO₂ reduction under visible light photocatalysis using porous NiO nanoparticles, an atypical metal oxide. *New J. Chem.* **46**: 10806-10813.
- D'Amario B, Perez C, Grelaud M, Pitta P, Krasakopoulou E, Ziveri P. 2020. Coccolithophore community response to ocean acidification and warming in the Eastern Mediterranean Sea: results from a mesocosm experiment. *Sci. Rep.* **10**: 12637.
- Stitt M, Lunn J, Usadel B. 2010. Arabidopsis and primary photosynthetic metabolism - more than the icing on the cake. *Plant J.* **61**: 1067-1091.
- Ragsdale SW, Pierce E. 2008. Acetogenesis and the Wood-Ljungdahl pathway of CO₂ fixation. *Biochim. Biophys. Acta.* **1784**: 1873-1898.
- Claassens NJ, Bordanaba-Florit G, Cotton CAR, De Maria A, Finger-Bou M, Friedeheim L, *et al.* 2020. Replacing the Calvin cycle with the reductive glycine pathway in *Cupriavidus necator*. *Metab. Eng.* **62**: 30-41.

20. Modde K, Timm S, Florian A, Michl K, Fernie AR, Bauwe H. 2017. High serine:glyoxylate aminotransferase activity lowers leaf daytime serine levels, inducing the phosphoserine pathway in Arabidopsis. *J. Exp. Bot.* **68**: 643-656.
21. Xu Y, Ren J, Wang W, Zeng AP. 2022. Improvement of glycine biosynthesis from one-carbon compounds and ammonia catalyzed by the glycine cleavage system in vitro. *Eng. Life Sci.* **22**: 40-53.
22. Gonzalez de la Cruz J, Machens F, Messerschmidt K, Bar-Even A. 2019. Core catalysis of the reductive glycine pathway demonstrated in yeast. *ACS Synth. Biol.* **8**: 911-917.
23. Hong Y, Arbter P, Wang W, Rojas LN, Zeng AP. 2021. Introduction of glycine synthase enables uptake of exogenous formate and strongly impacts the metabolism in *Clostridium pasteurianum*. *Biotechnol. Bioeng.* **118**: 1366-1380.
24. Sanchez-Andrea I, Guedes IA, Hornung B, Boeren S, Lawson CE, Sousa DZ, et al. 2020. The reductive glycine pathway allows autotrophic growth of *Desulfovibrio desulfuricans*. *Nat. Commun.* **11**: 5090.
25. Zarzycki J, Brecht V, Muller M, Fuchs G. 2009. Identifying the missing steps of the autotrophic 3-hydroxypropionate CO₂ fixation cycle in *Chloroflexus aurantiacus*. *Proc. Natl. Acad. Sci. USA* **106**: 21317-21322.
26. Huber H, Gallenberger M, Jahn U, Eylert E, Berg IA, Kockelkorn D, et al. 2008. A dicarboxylate/4-hydroxybutyrate autotrophic carbon assimilation cycle in the hyperthermophilic Archaeum *Ignicoccus hospitalis*. *Proc. Natl. Acad. Sci. USA* **105**: 7851-7856.
27. Hawkins AS, Han Y, Bennett RK, Adams MW, Kelly RM. 2013. Role of 4-hydroxybutyrate-CoA synthetase in the CO₂ fixation cycle in thermoacidophilic archaea. *J. Biol. Chem.* **288**: 4012-4022.
28. Loder AJ, Han Y, Hawkins AB, Lian H, Lipscomb GL, Schut GJ, et al. 2016. Reaction kinetic analysis of the 3-hydroxypropionate/4-hydroxybutyrate CO₂ fixation cycle in extremely thermoacidophilic archaea. *Metab. Eng.* **38**: 446-463.
29. Steffens L, Pettinato E, Steiner TM, Mall A, Konig S, Eisenreich W, et al. 2021. High CO₂ levels drive the TCA cycle backwards towards autotrophy. *Nature* **592**: 784-788.
30. Cheng HT, Lo SC, Huang CC, Ho TY, Yang YT. 2019. Detailed profiling of carbon fixation of in silico synthetic autotrophy with reductive tricarboxylic acid cycle and Calvin-Benson-Bassham cycle in *Escherichia coli* using hydrogen as an energy source. *Synth. Syst. Biotechnol.* **4**: 165-172.
31. Bar-Even A, Noor E, Lewis NE, Milo R. 2010. Design and analysis of synthetic carbon fixation pathways. *Proc. Natl. Acad. Sci. USA* **107**: 8889-8894.
32. Kerfeld CA. 2016. Rewiring *Escherichia coli* for carbon-dioxide fixation. *Nat. Biotechnol.* **34**: 1035-1036.
33. Antonovsky N, Gleizer S, Noor E, Zohar Y, Herz E, Barenholz U, et al. 2016. Sugar synthesis from CO₂ in *Escherichia coli*. *Cell* **166**: 115-125.
34. Gleizer S, Ben-Nissan R, Bar-On YM, Antonovsky N, Noor E, Zohar Y, et al. 2019. Conversion of *Escherichia coli* to generate all biomass carbon from CO₂. *Cell* **179**: 1255-1263 e1212.
35. Lee SY, Kim YS, Shin W-R, Yu J, Lee S, et al. 2020. Non-photosynthetic CO₂ bio-mitigation by *Escherichia coli* harbouring CBB genes. *Green Chem.* **22**: 6889-6896.
36. Flamholz AI, Dugan E, Blikstad C, Gleizer S, Ben-Nissan R, Amram S, et al. 2020. Functional reconstitution of a bacterial CO₂ concentrating mechanism in *Escherichia coli*. *Elife* **9**: 59882.
37. Woolston BM, King JR, Reiter M, Van Hove B, Stephanopoulos G. 2018. Improving formaldehyde consumption drives methanol assimilation in engineered *E. coli*. *Nat. Commun.* **9**: 2387.
38. He H, Edlich-Muth C, Lindner SN, Bar-Even A. 2018. Ribulose monophosphate shunt provides nearly all biomass and energy required for growth of *E. coli*. *ACS Synth. Biol.* **7**: 1601-1611.
39. Keller P, Noor E, Meyer F, Reiter MA, Anastassov S, Kiefer P, et al. 2020. Methanol-dependent *Escherichia coli* strains with a complete ribulose monophosphate cycle. *Nat. Commun.* **11**: 5403.
40. Kim S, Lindner SN, Aslan S, Yishai O, Wenk S, Schann K, et al. 2020. Growth of *E. coli* on formate and methanol via the reductive glycine pathway. *Nat. Chem. Biol.* **16**: 538-545.
41. Yu H, Liao JC. 2018. A modified serine cycle in *Escherichia coli* converts methanol and CO₂ to two-carbon compounds. *Nat. Commun.* **9**: 3992.
42. He H, Hoper R, Dodenhoft M, Marliere P, Bar-Even A. 2020. An optimized methanol assimilation pathway relying on promiscuous formaldehyde-condensing aldolases in *E. coli*. *Metab. Eng.* **60**: 1-13.
43. Jo BH, Kim IG, Seo JH, Kang DG, Cha HJ. 2013. Engineered *Escherichia coli* with periplasmic carbonic anhydrase as a biocatalyst for CO₂ sequestration. *Appl. Environ. Microbiol.* **79**: 6697-6705.
44. Kato A, Takatani N, Ikeda K, Maeda SI, Omata T. 2017. Removal of the product from the culture medium strongly enhances free fatty acid production by genetically engineered *Synechococcus elongatus*. *Biotechnol. Biofuels* **10**: 141.
45. Yunus IS, Wichmann J, Wordenweber R, Lauersen KJ, Kruse O, Jones PR. 2018. Synthetic metabolic pathways for photobiological conversion of CO₂ into hydrocarbon fuel. *Metab. Eng.* **49**: 201-211.
46. Yunus IS, Jones PR. 2018. Photosynthesis-dependent biosynthesis of medium chain-length fatty acids and alcohols. *Metab. Eng.* **49**: 59-68.
47. Choe H, Joo JC, Cho DH, Kim MH, Lee SH, Jung KD, et al. 2014. Efficient CO₂-reducing activity of NAD-dependent formate dehydrogenase from *Thiobacillus* sp. KNK65MA for formate production from CO₂ gas. *PLoS One* **9**: e103111.
48. Aslan AS, Valjakka J, Ruupinen J, Yildirim D, Turner NJ, Turunen O, et al. 2017. Chaetomium thermophilum formate dehydrogenase has high activity in the reduction of hydrogen carbonate (HCO₃⁻) to formate. *Protein Eng. Des. Sel.* **30**: 47-55.
49. Boldt A, Ansoerge-Schumacher MB. 2020. Formate dehydrogenase from *Rhodococcus jostii* (RjFDH) – A high-performance tool for NADH regeneration. *Adv. Synth. Catal.* **362**: 4109-4118.
50. Singh RK, Singh R, Sivakumar D, Kondaveeti S, Kim T, Li J, et al. 2018. Insights into cell-free conversion of CO₂ to chemicals by a multienzyme cascade reaction. *ACS Catal.* **8**: 11085-11093.
51. Kuk SK, Gopinath K, Singh RK, Kim TD, Lee Y, Choi WS, et al. 2019. NADH-free electroenzymatic reduction of CO₂ by conductive hydrogel-conjugated formate dehydrogenase. *ACS Catal.* **9**: 5584-5589.
52. Seelajaroen H, Bakandritsos A, Otyepka M, Zboril R, Sariciftci NS. 2020. Immobilized enzymes on graphene as nanobiocatalyst. *ACS Appl. Mater. Interfaces* **12**: 250-259.
53. Sharma T, Kumar A. 2021. Efficient reduction of CO₂ using a novel carbonic anhydrase producing *Corynebacterium flavescens*. *Environ. Eng. Res.* **26**: 200191.
54. Kanao T, Kawamura M, Fukui T, Atomi H, Imanaka T. 2002. Characterization of isocitrate dehydrogenase from the green sulfur bacterium *Chlorobium limicola*. A carbon dioxide-fixing enzyme in the reductive tricarboxylic acid cycle. *Eur. J. Biochem.* **269**: 1926-1931.
55. Katsyva A, Schoelmerich MC, Basen M, Muller V. 2021. The pyruvate:ferredoxin oxidoreductase of the thermophilic acetogen, *Thermoanaerobacter kivui*. *FEBS Open Bio* **11**: 1332-1342.
56. Gibson MI, Brignole EJ, Pierce E, Can M, Ragsdale SW, Drennan CL. 2015. The structure of an oxalate oxidoreductase provides insight into microbial 2-oxoacid metabolism. *Biochemistry* **54**: 4112-4120.
57. Chen PY, Li B, Drennan CL, Elliott SJ. 2019. A reverse TCA cycle 2-oxoacid:ferredoxin oxidoreductase that makes C-C bonds from CO₂. *Joule* **3**: 595-611.

58. Li B, Steindel P, Haddad N, Elliott SJ. 2021. Maximizing (Electro)catalytic CO₂ reduction with a ferredoxin-based reduction potential gradient. *ACS Catal.* **11**: 4009-4023.
59. Li B, Elliott SJ. 2016. The Catalytic Bias of 2-Oxoacid:ferredoxin Oxidoreductase in CO₂: evolution and reduction through a ferredoxin-mediated electrocatalytic assay. *Electrochim. Acta* **199**: 349-356.
60. Wayama F, Hatsugai N, Okumura Y. 2022. Bipyridines mediate electron transfer from an electrode to nicotinamide adenine dinucleotide phosphate. *PLoS One* **17**: e0269693.
61. Striepe L, Baumgartner T. 2017. Viologens and their application as functional materials. *Chem. Eur. J.* **23**: 16924-16940.
62. Bar-Even A, Flamholz A, Noor E, Milo R. 2012. Thermodynamic constraints shape the structure of carbon fixation pathways. *Biochim. Biophys. Acta* **1817**: 1646-1659.
63. El-Zahab B, Donnelly D, Wang P. 2008. Particle-tethered NADH for production of methanol from CO₂ catalyzed by coimmobilized enzymes. *Biotechnol. Bioeng.* **99**: 508-514.
64. Ren S, Wang Z, Bilal M, Feng Y, Jiang Y, Jia S, et al. 2020. Co-immobilization multienzyme nanoreactor with co-factor regeneration for conversion of CO₂. *Int. J. Biol. Macromol.* **155**: 110-118.
65. Ji X, Su Z, Wang P, Ma G, Zhang S. 2015. Tethering of nicotinamide adenine dinucleotide inside hollow nanofibers for high-yield synthesis of methanol from carbon dioxide catalyzed by coencapsulated multienzymes. *ACS Nano.* **9**: 4600-4610.
66. Marpani F, Sarossy Z, Pinelo M, Meyer AS. 2017. Kinetics based reaction optimization of enzyme catalyzed reduction of formaldehyde to methanol with synchronous cofactor regeneration. *Biotechnol. Bioeng.* **114**: 2762-2770.
67. Cazelles R, Drone J, Fajula F, Ersen O, Moldovan S, Galarneau A. 2013. Reduction of CO₂ to methanol by a polyenzymatic system encapsulated in phospholipids-silica nanocapsules. *New J. Chem.* **37**: 3721-3730.
68. Song H, Ma C, Liu P, You C, Lin J, Zhu Z. 2019. A hybrid CO₂ electroreduction system mediated by enzyme-cofactor conjugates coupled with Cu nanoparticle-catalyzed cofactor regeneration. *J. CO₂ Util.* **34**: 568-575.
69. Lee SY, Lim SY, Seo D, Lee J-Y, Chung TD. 2016. Light-driven highly selective conversion of CO₂ to formate by electrosynthesized enzyme/cofactor thin film electrode. *Adv. Energy Mater.* **6**: 1502207.
70. Yuan M, Sahin S, Cai R, Abdellaoui S, Hickey DP, Minter SD, et al. 2018. Creating a low-potential redox polymer for efficient electroenzymatic CO₂ reduction. *Angew. Chem. Int. Ed.* **57**: 6582-6586.
71. Reda T, Plugge CM, Abram NJ, Hirst J. 2008. Reversible interconversion of carbon dioxide and formate by an electroactive enzyme. *Proc. Natl. Acad. Sci. USA* **105**: 10654-10658.
72. Cai R, Milton RD, Abdellaoui S, Park T, Patel J, Alkhatini B, et al. 2018. Electroenzymatic C-C Bond Formation from CO₂. *J. Am. Chem. Soc.* **140**: 5041-5044.
73. Zhang L, Can M, Ragsdale SW, Armstrong FA. 2018. Fast and selective photoreduction of CO₂ to CO catalyzed by a complex of carbon monoxide dehydrogenase, TiO₂, and Ag nanoclusters. *ACS Catal.* **8**: 2789-2795.
74. Kim S, Giraldo N, Rainaldi V, Machens F, Collas F, Kubis A, et al. 2023. Optimizing *E. coli* as a formatrophic platform for bioproduction via the reductive glycine pathway. *Front. Bioeng. Biotechnol.* **11**: 1091899.
75. Davies KJ, Doroshov JH. 1986. Redox cycling of anthracyclines by cardiac mitochondria. I. Anthracycline radical formation by NADH dehydrogenase. *J. Biol. Chem.* **261**: 3060-3067.
76. Dutton PL, Moser CC, Sled VD, Daldal F, Ohnishi T. 1998. A reductant-induced oxidation mechanism for complex I. *Biochim. Biophys. Acta Bioenerg.* **1364**: 245-257.
77. Kay CJ, Barber MJ, Notton BA, Solomonson LP. 1989. Oxidation-reduction midpoint potentials of the flavin, haem and Mo-pterin centres in spinach (*Spinacia oleracea* L.) nitrate reductase. *Biochem. J.* **263**: 285-287.
78. Giastas P, Pinotsis N, Efthymiou G, Wilmanns M, Kyritsis P, Moulis J-M, et al. 2006. The structure of the 2[4Fe-4S] ferredoxin from *Pseudomonas aeruginosa* at 1.32-Å resolution: comparison with other high-resolution structures of ferredoxins and contributing structural features to reduction potential values. *J. Biol. Inorg. Chem.* **11**: 445-458.
79. Schipke CG, Goodin DB, McRee DE, Stout CD. 1999. Oxidized and reduced *Azotobacter vinelandii* ferredoxin I at 1.4 Å resolution: conformational change of surface residues without significant change in the [3Fe-4S]^{+/0} cluster. *Biochemistry* **38**: 8228-8239.
80. Yoch DC, Valentine RC. 1972. Four-iron (sulfide) ferredoxin from *Bacillus polymyxa*. *J. Bacteriol.* **110**: 1211-1213.
81. Giastas P, Pinotsis N, Efthymiou G, Wilmanns M, Kyritsis P, Moulis JM, et al. 2006. The structure of the 2[4Fe-4S] ferredoxin from *Pseudomonas aeruginosa* at 1.32-Å resolution: comparison with other high-resolution structures of ferredoxins and contributing structural features to reduction potential values. *J. Biol. Inorg. Chem.* **11**: 445-458.
82. Yoon KS, Bobst C, Hemann CF, Hille R, Tabita FR. 2001. Spectroscopic and functional properties of novel 2[4Fe-4S] cluster-containing ferredoxins from the green sulfur bacterium *Chlorobium tepidum*. *J. Biol. Chem.* **276**: 44027-44036.
83. Kyritsis P, Hatzfeld OM, Link TA, Moulis JM. 1998. The two [4Fe-4S] clusters in *Chromatium vinosum* ferredoxin have largely different reduction potentials. Structural origin and functional consequences. *J. Biol. Chem.* **273**: 15404-15411.
84. Saridakis E, Giastas P, Efthymiou G, Thoma V, Moulis JM, Kyritsis P, et al. 2009. Insight into the protein and solvent contributions to the reduction potentials of [4Fe-4S]^{2+/+} clusters: crystal structures of the *Allochromatium vinosum* ferredoxin variants C57A and V13G and the homologous *Escherichia coli* ferredoxin. *J. Biol. Inorg. Chem.* **14**: 783-799.
85. Bender G, Ragsdale SW. 2011. Evidence that ferredoxin interfaces with an internal redox shuttle in Acetyl-CoA synthase during reductive activation and catalysis. *Biochemistry* **50**: 276-286.
86. Breton JL, Duff JL, Butt JN, Armstrong FA, George SJ, Petillot Y, et al. 1995. Identification of the iron-sulfur clusters in a ferredoxin from the archaeon *Sulfolobus acidocaldarius*. Evidence for a reduced [3Fe-4S] cluster with pH-dependent electronic properties. *Eur. J. Biochem.* **233**: 937-946.
87. Boll M, Fuchs G, Tilley G, Armstrong FA, Lowe DJ. 2000. Unusual spectroscopic and electrochemical properties of the 2[4Fe-4S] ferredoxin of *Thaueria aromatica*. *Biochemistry* **39**: 4929-4938.
88. Abdul Wahab R, Wayama F, Hatsugai N, Okumura Y. 2022. Bipyridines mediate electron transfer from an electrode to nicotinamide adenine dinucleotide phosphate. *PLoS One* **17**: e0269693.